Simple and compact high-power continuous-wave deep ultraviolet source at 261 nm based on diode-pumped intra-cavity frequency doubled Pr:LiYF₄ green laser

KAI FENG,[1,2] DONG WANG,[1] YIZHEN ZHU,[1] BIN XU,[1,2,3,*] ZHONG CHEN,[1] MAURO LUCIANO BAESSO,[4] AND TOMAZ CATUNDA[5]

[1]*School of Electronic Science and Engineering, Xiamen University, Xiamen 361005, China*
[2]*Shenzhen Research Institute of Xiamen University, Shenzhen 518057, China*
[3]*Fujian Key Laboratory of Ultrafast Laser Technology and Applications, Xiamen 361005, China*
[4]*Departamento de Física, Universidade Estadual de Maringá, Maringá, PR 87020-900, Brazil*
[5]*Instituto de Física de Sao Carlos, Universidade de Sao Paulo, P.O. Box 369, Sao Carlos, SP 13560-970, Brazil*
[*]*xubin@xmu.edu.cn*

Abstract: We report the recent progress on diode-pumped high-power continuous-wave Pr:LiYF₄ (YLF) green laser and deep ultraviolet (DUV) laser generation via intracavity frequency doubling. Using two InGaN blue diode lasers as pump source to form a double-end pumping geometry, in this work, we have demonstrated a green laser at 522 nm with a maximum output power of 3.42 W, which is believed to be the highest power ever achieved in all-solid-state Pr^{3+} lasers in this specific spectral region. Moreover, by intracavity frequency doubling of the achieved green laser, we have further obtained a DUV laser at about 261 nm with a maximum output power of 1.42 W, which is far higher than previous results. The watt-level 261-nm laser paves the way towards the realization of simple and compact DUV source for a variety of applications.

1. Introduction

Ultraviolet (UV) lasers have been widely used in many fields [1–5], such as material processing, medicine, bacterial deactivation, semiconductor photolithography, laser spectroscopy, single-molecule imaging and optical characterization of materials. As a result, the pursuit towards simple, small-size and cost-effective UV sources has never stopped. In fact, UV source generation has always been an interesting and valuable research topic during the past decades. Among the UV sources, for a long time, all-solid-state UV laser has attracted a lot of attention because of its desirable advantages as compactness, robustness, long lifetime and high efficiency conversion. Cascaded frequency conversion (also called high-order harmonic) of near infrared (NIR) lasers mostly based on Nd^{3+} lasers operating in pulsed regime (Q switching or mode locking) by using nonlinear optical crystals is an effective way to obtain UV lasers, which have been widely explored in the past years [6–8]. However, on the one hand, frequency conversion at least twice is necessary, which indeed destroys the so-called advantages of all-solid-state lasers to a great extent. Moreover, in general, complicated amplification of the initial NIR sources is also necessary in order to achieve considerable UV output [6,8]. On the other hand, in comparison to pulsed UV lasers, the generation of continuous-wave (CW) UV lasers brings austerer challenges because of much reduced conversion efficiency under the siutation of low peak power. For CW UV lasers, a special cavity resonant enhancement technology has been developed to promote the conversion efficiency [9–11]. This technology has gain great success during the past years for generating CW UV lasers. Nevertheless, It should be noted that this technology is rather complicated and not easy to master. In addition, the whole UV laser system becomes much more complicated again.

In fact, frequency doubling provides the simplest and high-efficiency method for short wavelength laser generation. Therefore, if directly substituting all-solid-state visible lasers for Nd^{3+} NIR sources as fundamental laser, it should be completely possible to produce high-performance UV lasers and even deep UV (DUV) with advantages. With the development of InGaN blue diode laser as pump source, direct laser source in visible spectral region based on Pr^{3+} lasers is now becoming more and more developed. For instance, in 2011, Gün et al. reported rich laser radiations in Pr:YLF crystal with a green laser power of 773 mW at about 522 nm [12]. In 2016, we improved the green laser power to 1.7 W [13]. In 2018, the green laser was power increased to 1.8 W by Tanaka et al. [14]. Recently, in 2019, Fujita et al. [15] demonstrated the Pr:YLF green laser again with a maximum output power of 1.1 W.

Frequency doubling of all-solid-state Pr^{3+} lasers for UV and DUV laser generation has also been paid much attention since the very initial stage of blue diode pumped Pr^{3+} lasers. In 2006, i.e. two years after the first diode-pumped Pr^{3+} laser, Richter et al. investigated a Pr:YLF-LBO laser at 320 nm [16]. For this 320-nm ultraviolet laser, recent research has increased the output power to 1.01 W [17], and then further increased it to 3.22W [18], which exhibits excellent merit of diode-pumped intracavity frequency doubled Pr^{3+} lasers. The merit has been further extended by frequency doubling of green Pr^{3+} laser for simple and compact DUV laser generation. In 2011, Gün et al. reported a high-performance diode-pumped Pr:YLF-BBO laser at 261 nm with a maximum output power of 481 mW [19], which is still the highest output power of diode-pumped Pr^{3+}-based DUV continuous-wave laser. In history, it should be pointed out that 469-nm Nd:YAG-LBO laser and 479-nm optically pumped semiconductor laser (OPSL) have also been used as pump sources [20–22]. Using an OPSL as pump source, more than 4-W of the Pr:YLF green laser and about 1-W of the 261 nm DUV laser have been achieved [23]. However, due to the lack of advantages that semiconductor lasers possess, these pump sources will eventually withdraw from the historical stage.

In this work, we have improved the continuous-wave output powers of diode-pumped Pr:YLF green laser at 522 nm and its frequency doubling to 261 nm to the highest level that has never been demonstrated previously with respect to the all-solid-state Pr^{3+}-based lasers.

2. Experimental setup

The laser experimental setup is schematically shown in Fig. 1 (Fig. 1(a) is for green laser generation and Fig. 1(b) is for 261 nm DUV laser generation). Two InGaN blue diode lasers emitting at about 444 nm at maximum output power of 6.5 W were used as pump sources. Beam propagation factor of the blue pump laser was measured to be approximately 4.8 and 25.5 in x and y directions. Pump beam of the two pump sources were collected into the laser gain medium by two 75-mm (focal length) aspheric plane-convex lenses from two sides of the gain medium to form double end pumping geometry. After focusing, in the x and y directions, the intensity distribution of the waist spot of the pump beam is very close to the Gaussian mode, and the spot size is about 130 and 284 µm, respectively. For green laser operation, a V-shaped cavity with two flat mirrors (M1 and M2) and a concave mirror (M3) was arranged. The M1 and M2 mirrors have the same coating as about 95% transmission at pumping wavelength and 99.9% high reflection at the green wavelength. For suppressing the high-gain red emission at about 639 nm, the two mirrors also have high transmissions of more than 80% at the red wavelength, which ensures that only the considered green emission can be lased. The curved M3 mirror with ROC of 100 mm played the role of output coupler and its transmission is about 2.0% at 522 nm. Here, note that we have not made efforts to optimize the transmission for best green laser performance. The used one was just available presently in our lab. For intracavity frequency doubling, we arranged a Z-type cavity. The M4 mirror with ROC of 100 mm has 99.9% high reflection at green and about 95% high transmission at 261 nm. The flat M5 mirror has high reflections of 99.9% and 99.5% at green and 261 nm, respectively. Thus, according to the coating, the M4 mirror plays a role as

output coupler of the 261 nm DUV laser. It should be pointed out that the flat mirror (M2) does not introduce astigmatism, so the V-shaped cavity used for green laser experiment is essentially a plane-concave two mirror linear cavity, while the Z-shaped cavity used for frequency doubling is essentially a V-shaped cavity. The function of M2 here is to facilitate the focusing and coupling of the pump laser at the right side into the Pr:YLF crystal.
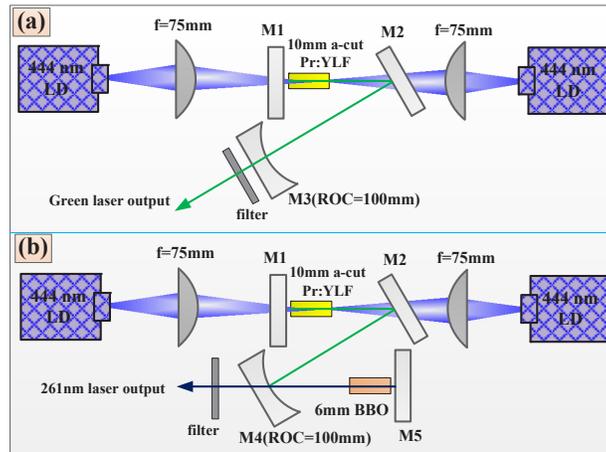

Fig. 1. Experimental setup of diode-pumped continuous-wave (a) Pr:YLF green laser and (b) Pr:YLF-BBO DUV laser.

The laser gain medium is a 0.3at.% doped a-cut Pr:YLF single crystal with aperture of 3×3 mm^2 and length of 10 mm. Thus, the crystal absorbed about 85% of the total pump power. Moreover, in order to reduce the Fresnel loss and improve the laser performance, the Pr:YLF crystal was anti-reflection coated. In addition, in order to effectively remove the heat loading inside the laser crystal, we wrapped it with indium foil and then mounted it inside a copper block. The copper block was connected to a water cooling chiller with temperature set at 12 °C. During intracavity frequency doubling, a BBO crystal with length of 6 mm, designed for type I critical phase matching ($\theta=48.9°$, $\varphi=0$) and AR coated at 522 nm and 261 nm, was placed in the beam waist located very close to the M5 mirror. The optimal operating temperature of the BBO crystal is at room temperature of about 25 °C, which was managed by a thermoelectric controller for active temperature control.

3. Results and discussion

The polarization-dependent emission spectra of the Pr:YLF crystal under the excitation of a 444-nm diode laser is shown in Fig. 2. For Pr:YLF crystal, the most intense emission locates at red line of about 639.5 nm with emission cross section of 22.3×10^{-20} cm^2. However, emission intensity of the green line with peak at about 522.56 nm, corresponding to emission transition from $^3P_1$ to $^3H_5$, is relatively very weak and its emission cross section is only about 2.2×10^{-20} cm^2, i.e. about one tenth of that of the 639.5-nm emission. This is one of the reasons that diode-pumped Pr^{3+} green laser has been power limited to only 1.8 W and its frequency doubled operation at 261 nm DUV has also been power limited to less than 0.5 W presently.

After a good alignment of the V-shaped cavity for fundamental wave operation, we achieved a maximum output power up to 3.43 W at an absorbed power of 10.38 W by using the 2.0% transmitted mirror, as shown in Fig. 3. This is almost twofold of the previous result as reported in Ref. [14]. Moreover, According to Ref. [13], the optimized transmission of the output coupler with respect to the green emission should be about 3%. Therefore, it is reliable to believe that the
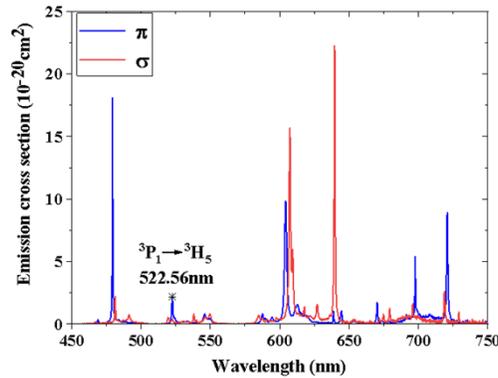
Fig. 2. Polarization-dependent emission spectra of Pr:YLF crystal using a 444-nm blue diode laser as excitation source.

maximum output power could be further improved to more than 4 W under optimal condition. In addition, threshold of the green laser is about 0.22 W of absorbed power. From the threshold to the maximum output power, the laser has not shown any power saturation phenomenon. The laser output power shows very good linearity with a slope efficiency of about 33.8% with respect to the absorbed power. Frankly, the efficiency is not high and we previously reported a 49% slope efficiency [13]. According to our estimation, in this present work, the overlap efficiency between pump beam and cavity mode is about 71.5%, while the previous overlap efficiency is about 82.3%. It is understandable if we take the pump beam quality into account. In our previous work, we used a relatively low power pump source with good beam quality that is advantageous to achieve high overlap efficiency for high-efficiency laser operation. However, in this present work, in order to achieve higher output power, pump source with higher output power is necessary. Unfortunately, for the present diode laser without fiber coupling, the higher the power is, the worse the beam quality is. In addition, the laser wavelength of the green emission is also shown in Fig. 3 as an inset with a peak at 522.56 nm.
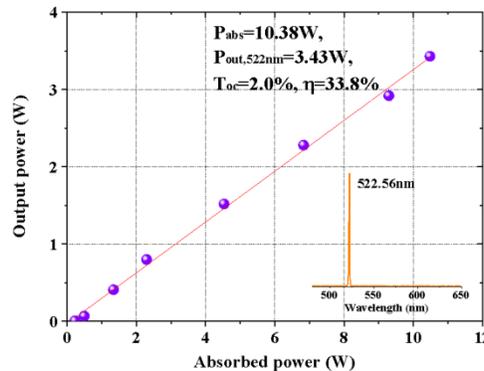

Fig. 3. Output power of diode-pumped continuous-wave Pr:YLF laser at green; inset: wavelength of the green laser.

We estimate the intracavity round-trip loss L by using the following expression

$$\eta_s = \frac{\lambda_p}{\lambda_o} \eta_p \frac{T}{T+L} \tag{1}$$

where η_s is the slope efficiency; λ_p and λ_o are the pumping wavelength and laser wavelength, respectively; η_p is the excitation quantum efficiency, i.e. the fraction of excited ions per absorbed pump photons, which can be assumed to be equal to unity; T is the transmission of output couplers; L is the intracavity round-trip loss. Substituting the values into this expression, we can readily calculate the intracavity round-trip loss to be about 3.0%.

We measured the output power stability of the green laser at maximum output power, as shown in Fig. 4(a). In 20 minutes, the maximum output power was measured to have an average of about 3.37 W. As a result, the power stability was estimated to be about 0.77% with respect to the average power. The stability is about 1.50% corresponding to the maximum output power. Hence, we can safely arrive at a conclusion that the diode-pumped Pr:YLF green laser exhibits a good power stability and the good power stability indicates at least a weak mode competition. During the experiment, by monitoring the laser wavelength, we found that the peak wavelength always keeps the same and there is no significant change in the longitudinal mode structure. Furthermore, we measured the transverse mode by using a WinCamD-LCM CMOS beam profiling camera (DataRay Inc.). Figure 4(b) shows the beam spot size of the green laser at different distance, which was focused by a positive lens with focal length of 75 mm. By fitting the data, we can deduce the beam propagation factor M^2 to be about 1.78 and 2.45 in x and y directions. We think that the thermal lensing effect was not strong inside the laser crystal. The insets in Fig. 4(b) shows the typical beam spot at maximum output power.
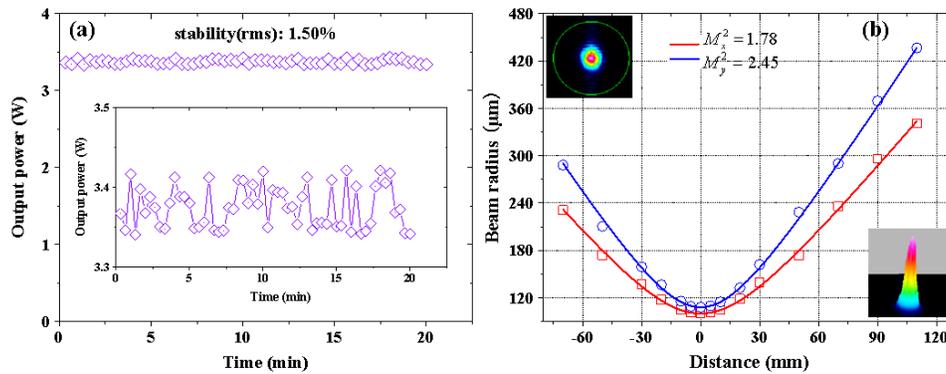

Fig. 4. (a) Maximum output power stability of the Pr:YLF green laser in 20 minutes; inset: enlarging the output power coordinator around 3.4 W and (b) M^2 factors characterization of the Pr:YLF green laser for evaluating the beam quality by measuring the beam sizes at different distances; inset: 2D and 3D beam spots.

In the experiment, we have also made efforts to operate intracavity frequency doubling of the Pr:YLF green laser. As we mentioned, in comparison to fourth harmonic generation of Nd^{3+} NIR lasers, it provides the simplest method for generating DUV laser. Inserting the BBO nonlinear crystal into the Z-shaped cavity, the DUV laser can be readily observed with an UV sensor card. We, in Fig. 5, show the laser performance of the DUV laser. The maximum output power was found to be 1.42 W at the absorbed power of 10.38 W. The DUV laser wavelength was registered to have a peak at about 261 nm. In Fig. 5, we also show the modeling curve of the 261 nm DUV laser based on the Smith's analysis [24]. In the model, assuming that the pump power induces no thermal effect for the laser medium, then output power of frequency doubled laser can be written as

$$P_{2\omega} = \frac{\pi\omega_1^2}{8k}I_{sat}^2\left\{-\left[k+\frac{L_i}{I_{sat}}\right]+\left[\left(k+\frac{L_i}{I_{sat}}\right)^2+4\frac{k}{I_{sat}}(2K_cP_a-L_i)\right]^{\frac{1}{2}}\right\}^2 \quad (2)$$

here K_c and L_i are the pump coupling coefficient and the resonator loss. They can be deduced to be about 0.5 and 0.03, respectively, according to the fundamental wave laser experiment. I_{sat} is saturation intensity of the Pr:YLF crystal and parameter k is the effective nonlinearity of the BBO nonlinear crystal, which can be expressed as

$$k = \frac{4\pi^2}{\lambda_\omega^2} Z_0 \frac{d_{eff}^2 l^2}{n_2^3} \frac{\omega_1^2}{\omega_2^2} \beta \tag{3}$$

where $Z_0 = 377\ \Omega$ is the vacuum impedance, l is the length of the BBO crystal, which is 6 mm, $n_2 = 1.78$ is the refractive index at 261 nm, w_1 and w_2 are the beam waists in the Pr:YLF and BBO, respectively, and β (~4) is a factor that takes into account the phase mismatch between the fundamental and the second harmonic wave in the second pass in the BBO crystal. Since the $P_{2\omega}$ expression has nothing to do with thermal effect and the fact is that the thermal effect is not avoidable due to nonradiative decay, we, in order to reflect the real situation and present a good simulation, therefore add a monotonously increasing extra loss into the intracavity round-trip loss. In this work, we found a good agreement between the experimental data and modeling curve, as shown in Fig. 5, when the extra loss was finally increased to 0.023. That is to say, at the maximum output power, the intracavity round-trip loss was about 0.053. The extra loss should be mainly attributed to the insertion loss arising from the BBO crystal.
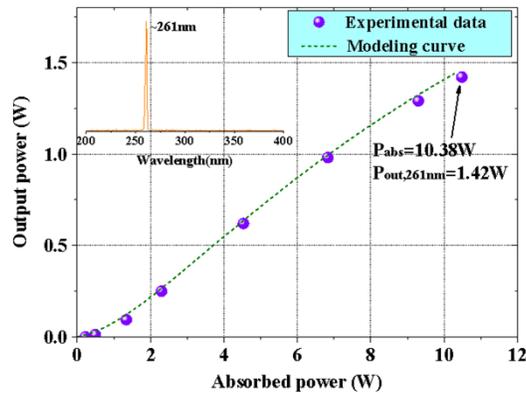

Fig. 5. Experimental data and modeling curve of the output power of Pr:YLF-BBO DUV laser at 261 nm; inset: wavelength of the DUV laser.

Figure 6(a) shows the output power stability of the 261 nm DUV laser. In 20 minutes, at the full pump power, the maximum output power was averaged to be 1.37 W, i.e. about 3.5% reduction corresponding to the highest output power of 1.42 W. Then, the stability was estimated to be about 1.49% with respect to the average maximum output power, while the stability was found to be about 3.17% with respect to the maximum output power. From the inset in Fig. 6(a), we can better see the detail of power fluctuation. During the 20-minute measurement time, we have not observed significant power degradation. However, it should be pointed out that BBO crystal has been found to exhibit UV absorption increased with time due to the formation of an absorption center at a peak power density of 55 MW/cm² [25], which will in turn lead to a decrease in UV laser power. However, due to our continuous-wave power intensity being far less than the reported value (only about 0.03 MW/cm²), we have not yet reached the level of forming so-called absorption centers in BBO crystals, and therefore no significant power reduction has been observed for at least 20 minutes of our measurement time.

In Fig. 6(b), we show the beam quality measurement by using a BC106-UV camera beam profiler (Thorlabs Inc.). Using the expression of beam propagation factor to fitting the experimental data,
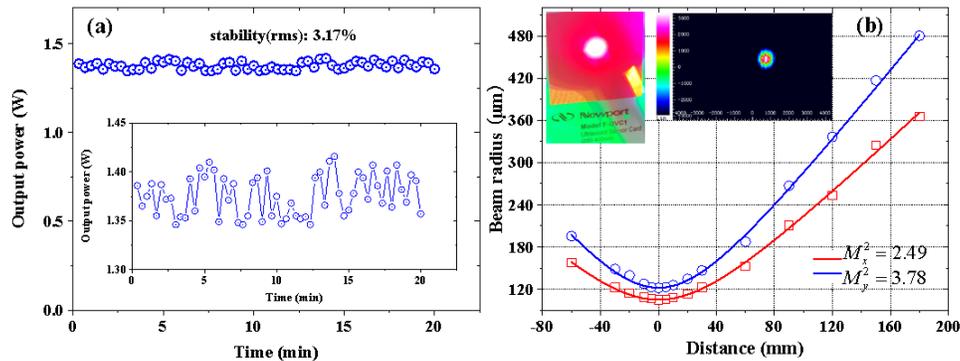
Fig. 6. (a) Maximum output power stability of the Pr:YLF-BBO DUV laser in 20 minutes; inset: enlarging the output power coordinator around 1.4 W and (b) M^2 factors characterization of the Pr:YLF-BBO DUV laser for evaluating the beam quality by measuring the beam sizes at different distances; inset: UV sensor card captured beam spot and CCD captured beam spot.

we deduced the M^2 factors in *x* and *y* directions to be about 2.49 and 3.78, respectively. The noncircular beam spot should be ascribed to the walk-off angle of the BBO crystal.

4. Conclusion

High order harmonic of NIR lasers is a complicated method for generating DUV radiation. Intracavity frequency doubling of InGaN diode-pumped Pr^{3+} laser at green for DUV generation is still at low developing level. Under this research background, in this work, we have investigated all-solid-state Pr:YLF green laser at 522 nm with a record maximum output power of 3.43 W. Then, using a BBO nonlinear crystal, we have operated intracavity frequency doubled laser at 261 nm with a record maximum output power of 1.42 W. The record breaking results here are all for all solid-state Pr^{3+} lasers. Such simple and compact DUV source could be very promising in a variety of applications. Last but not least, to improve the DUV laser efficiency, three aspects need to be addressed. First of all, increasing power density of the green laser in the cavity can be achieved by further increasing the pump power and improving the mode matching between the pump beam and the fundamental mode spot in the cavity. Moreover, no obvious thermal induced power rollover phenomenon was observed in this work, which means that the thermal effect is not very significant, indicating that the pump power we injected can be further improved for power scaling. In addition, according to Ref. [18], the damage threshold of a 0.15% doped Pr:YLF is close to about 20 W of absorbed power, far higher than the absorbed power in this present work. Therefore, power scaling of the considered green and DUV lasers by increasing pump power should be very feasible. Secondly, the length of the frequency doubling crystal should be precisely optimized. Finally, the average spot size of the fundamental mode spot in the frequency doubling crystal should also be precisely optimized. Comprehensive consideration should be given to ultimately improve the efficiency of the DUV laser.

Disclosures. The authors declare no conflicts of interest.

Data availability. Data underlying the results presented in this paper are not publicly available at this time but may be obtained from the authors upon reasonable request.

References

1. C. T. Pan, Y. M. Hwang, and C. W. Hsieh, "Fast fabrication of silicon based microstructures using 355 nm UV laser," Mater. Sci. Technol. **21**(11), 1344–1348 (2005).
2. Y. Ooka, T. Tetsumoto, A. Fushimi, W. Yoshiki, and T. Tanabe, "CMOS compatible high-Q photonic crystal nanocavity fabricated with photolithography on silicon photonic platform," Sci. Rep. **5**(1), 11312 (2015).
3. S. Orthaus, M. König, T. Schönau, V. Buschmann, S. Tannert, C. Lauritsen, F. Koberling, U. Ortmann, and R. Erdmann, "Crossing the Limit Towards Deep UV," Opt. Photonik **8**(1), 33–36 (2013).
4. L. I. Isaenko, A. Dragomir, J. G. McInerney, and D. N. Nikogosyan, "Anisotropy of two-photon absorption in BBO at 264 nm," Opt. Commun. **198**(4-6), 433–438 (2001).
5. Q. Fu, N. Hanrahan, L. Xu, S. Lane, D. Lin, Y. Jung, S. Mahajan, and D. Richardson, "High-power, high-efficiency, all-fiberized-laser-pumped, 260-nm, deep-UV laser for bacterial deactivation," Opt. Express **29**(26), 42485 (2021).
6. Q. Liu, X. Yan, M. Gong, H. Liu, G. Zhang, and N. Ye, "High-power 266 nm ultraviolet generation in yttrium aluminum borate," Opt. Lett. **36**(14), 2653 (2011).
7. L. Deyra, I. Martial, J. Didierjean, F. Balembois, and P. Georges, "Deep-UV 236.5 nm laser by fourth-harmonic generation of a single-crystal fiber Nd:YAG oscillator," Opt. Lett. **39**(8), 2236–2239 (2014).
8. Y. Chu, X. Zhang, B. Chen, J. Wang, J. Yang, R. Jiang, and M. Hu, "Picosecond high-power 213-nm deep-ultraviolet laser generation using β-BaB₂O₄ crystal," Opt. Laser Technol. **134**, 106657 (2021).
9. M. Oka, L. Y. Liu, W. Wiechmann, N. Eguchi, and S. Kubota, "All Solid-state Continuous-Wave Frequency-Quadrupled Nd:YAG Laser," IEEE J. Sel. Top. Quantum Electron. **1**(3), 859–866 (1995).
10. M. Scheid, F. Markert, J. Walz, J. Wang, M. Kirchner, and T. W. Hänsch, "750 mW continuous-wave solid-state deep ultraviolet laser source at the 253.7 nm transition in mercury," Opt. Lett. **32**(8), 955 (2007).
11. J. C. Shaw, S. Hannig, and D. J. Mccarron, "Stable 2 W continuous-wave 261.5 nm laser for cooling and trapping aluminum monochloride," Opt. Express **29**(23), 37140 (2021).
12. T. Gün, P. Metz, and G. Huber, "Power scaling of laser diode pumped Pr³⁺:LiYF₄ cw lasers: efficient laser operation at 522.6 nm, 545.9 nm, 607.2 nm, and 639.5 nm," Opt. Lett. **36**(6), 1002 (2011).
13. S. Luo, X. Yan, Q. Cui, B. Xu, H. Xu, and Z. Cai, "Power scaling of blue-diode-pumped Pr:YLF lasers at 523.0, 604.1, 606.9, 639.4, 697.8 and 720.9 nm," Opt. Commun. **380**, 357–360 (2016).
14. H. Tanaka, S. Fujita, and F. Kannari, "High-power visibly emitting Pr³⁺:YLF laser end pumped by single-emitter or fiber-coupled GaN blue laser diodes," Appl. Opt. **57**(21), 5923 (2018).
15. S. Fujita, H. Tanaka, and F. Kannari, "Intracavity second-harmonic pulse generation at 261 and 320 nm with a Pr³⁺:YLF laser Q-switched by a Co²⁺:MgAl₂O₄ spinel saturable absorber," Opt. Express **27**(26), 38134 (2019).
16. A. Richter, N. Pavel, E. Heumann, G. Huber, D. Parisi, A. Toncelli, M. Tonelli, A. Diening, and W. Seelert, "Continuous-wave ultraviolet generation at 320 nm by intracavity frequency doubling of red-emitting Praseodymium lasers," Opt. Express **14**(8), 3282 (2006).
17. Y. Zhang, J. Zou, W. Zheng, K. Feng, B. Xu, and Z. Yu, "Watt-level continuous-wave intracavity frequency-doubled Pr:YLF-LBO laser at 320 nm," Chin. Opt. Lett. **19**(9), 091406 (2021).
18. T. Zhang, W. Zheng, K. Feng, D. Wang, B. Xu, Z. Luo, Z. Yu, X. Cui, M. L. Baesso, and T. Catunda, "Towards Power Scaling of Simple CW Ultraviolet via Pr:LiYF₄-LBO Laser at 320 nm," IEEE Photonics Technol. Lett. **34**(2), 129–132 (2022).
19. T. Gün, P. Metz, and G. Huber, "Efficient continuous wave deep ultraviolet Pr³⁺:LiYF₄ laser at 261.3 nm," Appl. Phys. Lett. **99**(18), 181103 (2011).
20. B. Xu, P. Camy, J. L. Doualan, Z. Cai, and R. Moncorgé, "Visible laser operation of Pr³⁺-doped fluoride crystals pumped by a 469 nm blue laser," Opt. Express **19**(2), 1191 (2011).
21. W. Bolaños, G. Brasse, F. Starecki, A. Braud, J. L. Doualan, R. Moncorgé, and P. Camy, "Green, orange, and red Pr³⁺:YLiF₄ epitaxial waveguide lasers," Opt. Lett. **39**(15), 4450 (2014).
22. P. W. Metz, F. Reichert, F. Moglia, S. Müller, D. T. Marzahl, C. Kränkel, and G. Huber, "High-power red, orange, and green Pr³⁺:LiYF₄ lasers," Opt. Lett. **39**(11), 3193 (2014).
23. V. Ostroumov and W. Seelert, "1 W of 261 nm cw generation in a Pr3+:LiYF4 laser pumped by an optically pumped semiconductor laser at 479 nm," Proc. SPIE **6871**, 68711K (2008).
24. R. Smith, "Theory of intracavity optical second-harmonic generation," IEEE J. Quantum Electron. **6**(4), 215–223 (1970).
25. K. Takachiho, M. Yoshimura, Y. Takahashi, M. Imade, T. Sasaki, and Y. Mori, "Ultraviolet laser-induced degradation of CsLiB₆O₁₀ and β-BaB₂O₄," Opt. Mater. Express **4**(3), 599 (2014).